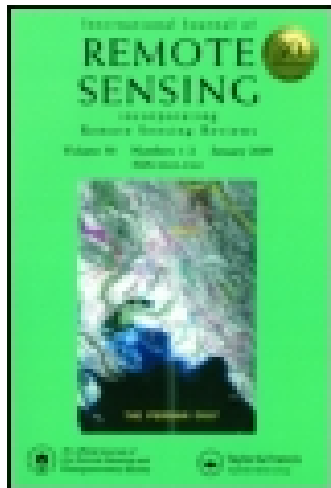


This article was downloaded by: [University of Sussex Library]

On: 18 January 2015, At: 03:54

Publisher: Taylor & Francis

Informa Ltd Registered in England and Wales Registered Number: 1072954 Registered office: Mortimer House, 37-41 Mortimer Street, London W1T 3JH, UK



International Journal of Remote Sensing

Publication details, including instructions for authors and subscription information:
<http://www.tandfonline.com/loi/tres20>

The U.K. EODC ERS-1 altimeter oceans processing scheme

R. T. TOKMAKIAN^a, P. G. CHALLENGOR^a, T. H. GUYMER^a & M. A. SROKOSZ^a

^a James Rennell Centre for Ocean Circulation, Gamma House, Chilworth Research Centre, Chilworth, Southampton, England, SO1 7NS, U.K

Published online: 07 May 2007.

To cite this article: R. T. TOKMAKIAN, P. G. CHALLENGOR, T. H. GUYMER & M. A. SROKOSZ (1994) The U.K. EODC ERS-1 altimeter oceans processing scheme, *International Journal of Remote Sensing*, 15:4, 939-962, DOI: [10.1080/01431169408954126](https://doi.org/10.1080/01431169408954126)

To link to this article: <http://dx.doi.org/10.1080/01431169408954126>

PLEASE SCROLL DOWN FOR ARTICLE

Taylor & Francis makes every effort to ensure the accuracy of all the information (the "Content") contained in the publications on our platform. However, Taylor & Francis, our agents, and our licensors make no representations or warranties whatsoever as to the accuracy, completeness, or suitability for any purpose of the Content. Any opinions and views expressed in this publication are the opinions and views of the authors, and are not the views of or endorsed by Taylor & Francis. The accuracy of the Content should not be relied upon and should be independently verified with primary sources of information. Taylor and Francis shall not be liable for any losses, actions, claims, proceedings, demands, costs, expenses, damages, and other liabilities whatsoever or howsoever caused arising directly or indirectly in connection with, in relation to or arising out of the use of the Content.

This article may be used for research, teaching, and private study purposes. Any substantial or systematic reproduction, redistribution, reselling, loan, sub-licensing, systematic supply, or distribution in any form to anyone is expressly forbidden. Terms & Conditions of access and use can be found at <http://www.tandfonline.com/page/terms-and-conditions>

The U.K. EODC ERS-1 altimeter oceans processing scheme

R. T. TOKMAKIAN, P. G. CHALLENGOR, T. H. GUYMER and
M. A. SROKOSZ†

James Rennell Centre for Ocean Circulation, Gamma House, Chilworth
Research Centre, Chilworth, Southampton SO1 7NS, England, U.K.

Abstract. This paper outlines the processing scheme for ERS-1 altimeter ocean products at the U.K. Earth Observation Data Centre (EODC). Central to the scheme is the use of Maximum Likelihood Estimation (MLE) to derive accurate geophysical information from the altimeter return waveforms. The output of the MLE is used, together with other algorithms and external data, to produce wind and wave, and sea surface topography products. Examples are given, based on Geosat data, of some possible applications of the ocean data that will be obtained from the ERS-1 altimeter.

1. Introduction

This paper describes the processing scheme for ERS-1 altimeter ocean products at the EODC, the philosophy that led to the adoption of that scheme, and some applications of the oceanographic data obtained from radar altimetry. We will review briefly what has been done for previous altimetric missions and then show how the EODC scheme for ERS-1 differs. The underlying goal of the approach is to extract the maximum amount of geophysical information from the radar altimeter return over the ocean surface.

One of the primary reasons for flying radar altimeters in space is to make global measurements of the ocean surface topography, from which, under the assumption of geostrophy, the surface currents can be calculated. Additionally, information on the significant wave height and sea surface wind speed can also be derived from the radar return. How this is done is described in more detail below. Clearly such measurements are important to studies of the global climate system, and the role of the oceans, and to more immediate concerns such as offshore operations and wave forecasting.

Prior to ERS-1 and Topex-Poseidon, four altimeters have been flown in space; an experimental one on Skylab in 1973, one on GEOS-3 from 1975 to 1978 (which, due to the lack of an on-board tape recorder only gave limited data coverage), one on Seasat in 1978 (which failed after 100 days of operation) and one on the U.S. Navy satellite Geosat which operated successfully from March 1985 to January 1990 (the height data from the first 18 months of this mission are classified and not available for scientific analysis). More details of these missions and results from them may be found in the special issues of: the *Journal of Geophysical Research*, **84**(B8), 1979 [GEOS-3], **87**(C5), 1982 and **88**(C3), 1983 [Seasat], **95**(C3), 1990 and **95**(C10), 1990

†M. A. Srokosz is a member of the NERC/BNSC Remote Sensing Applications Development Unit.

[Geosat]; the *I.E.E. Journal of Oceanic Engineering*, OE-5 (no. 2), 1980 [Seasat]; the *Johns Hopkins APL Technical Digest*, 8 (no. 2), 1987 [Geosat].

For all these missions the estimation of the oceanographic parameters was done by on-board processing of the radar return, with additional corrections being carried out once the parameters had been transmitted to the ground. The end result is the classic Geophysical Data Record (GDR), containing values of the parameters at one second intervals (corresponding to measurements approximately every seven kilometres along the ground track). The GDR data are distributed to users for further analysis. To achieve on-board (real-time) processing of the radar return with limited computational capability, some simplifying assumptions have to be made about the nature of the return. This enables three pieces of information to be derived from the return: the travel time of the pulse (giving the height of the satellite above the sea surface), the slope of the leading edge of the return (giving the significant wave height H_s), and the backscattered power σ^0 (related, via the mean square slope of the waves, to the wind speed near the sea surface). ERS-1 has a similar on-board processing scheme and the data transmitted to ground form the basis of the Fast Delivery products (available to users within 3 hours of acquisition). The on-board estimation of the parameters is based on a model of the return due to Brown (1977); (see also Barrick 1972) which assumes Gaussian statistics for the waves at the sea surface.

In reality the statistics of the waves at the sea surface are non-Gaussian (Barrick and Lipa 1985, Srokosz 1986). Therefore the on-board estimates do not give all the information contained in the return. To obtain the maximum amount of geophysical information, it is necessary to re-analyse the return signal on the ground. The ERS-1 radar altimeter transmits pulses at 1020 Hz and the on-board processor averages the returns in groups of 50 to give ~ 20 Hz waveforms (that is, the return signal measured in 64 'gates'; see Cudlip and Milnes 1994, this issue), from which it provides estimates of the geophysical parameters. These, together with the waveforms, are recorded and later transmitted to the Earth. For Seasat and Geosat, similar data (at 10 Hz) were transmitted to the ground, but the ocean waveforms were not re-analysed (except for specific, limited studies; Lipa and Barrick 1981, Hayne and Hancock 1990).

The processing scheme described in this paper has as its central feature the use of a Maximum Likelihood Estimation (MLE) method to derive geophysical parameters from ERS-1 waveforms on a routine basis. Use of a technique such as MLE is necessary as the waveform is noisy due to 'fading noise' affecting the return (Ulaby *et al.* 1982). MLE allows the fitting of a model return (a function of the parameters that are to be estimated) to the waveform, taking into account the known statistics of the fading noise. This leads, firstly, to more accurate estimates of the geophysical parameters of interest than those that are obtained from on-board processing, and secondly, to the possibility of estimating extra parameters in addition to those obtained by the on-board processor. The model return that is fitted to the waveforms is based on the assumption that the waves at the sea surface have non-Gaussian statistics (see below §§3 and 5, and also Srokosz 1986 b).

In what follows, we outline the processing scheme and the products in §2. Then, in §3, a description of the MLE is given, together with the results from studies in which it was applied to simulated waveform data. Section 4 discusses the algorithms used to produce the wind and wave information and their physical basis. This is followed, in §5, by a similar description of the sea surface topography algorithms.

Finally, in §6, we discuss example applications of the oceanographic data that will be obtained by the ERS-1 radar altimeter and some issues related to the calibration and validation of that data. A discussion of the products available from the EODC are given in a paper by Peters *et al.* (1994).

2. Processing scheme and products

At an early stage it was decided to produce, routinely, a number of parameters that had been developed since the launch of Seasat in 1978. These are mainly wave parameters and will be described in §4. It is hoped that these will make the altimeter wave data accessible to a larger applications community. One consequence of this is that the number of variables per record became too great for a single Geophysical Data Record (GDR) as produced for Seasat and Geosat (see, for example, Cheney *et al.* 1987) and proposed for Topex-Poseidon. The decision was taken to split the data into three products each of which would contain a subset of the full parameter set. These are the Basic Wind/Wave Product, the Advanced Wind/Wave Product and the Sea Surface Topography Product. Each is designed to serve a different section of the user community. We will now describe each product and suggest which communities they are particularly useful for.

The Basic Wind/Wave Product is intended to be used by the non-research wave user, the off-shore industry, for example. In addition to quality flags, time and position data, it contains the values of significant wave height (H_s), wind speed at 10 metres above the sea surface (assuming neutral stability) (U_{10}), mean square slope of the sea surface (s^2), friction velocity (u_*) derived from the bulk formula (Large and Pond 1982) and normalised radar cross-section (σ^0). All these data are at a sampling frequency of 1 Hz (equivalent to a ground track spacing of ~ 6.6 km) and the standard deviation and the number of good data points in the last second are included as measures of accuracy and for quality control purposes. The two parameters included here which were not on either of the Seasat and Geosat GDR's are the mean square slope and friction velocity (the Geosat GDR did not contain wind speed because of the difficulty in deciding on a suitable algorithm). The processing chain for this product is shown in figure 1 (a).

The Advanced Wind/Wave Product is designed for the research user or those requiring more detail than is given in the Basic Product. Figure 1 (b) shows the processing chain. The data are given at 20 Hz (the frequency at which data are transferred from the satellite). The parameters given are H_s and its standard deviation, mean square slope, σ^0 and its standard deviation, sea surface skewness (λ) and its standard deviation, U_{10} , the fourth spectral moment (m_4), wave period (T_A), percentage of waves breaking, minimum swell height (H_{\min}) and friction velocity derived directly from σ^0 , as opposed to the u_* in the Basic Wind/Wave Product which is derived via the bulk formulae. These new parameters will be described in greater detail in §4. The standard deviations given in this product do not come from the variation of the measured values as in the Basic Product, but are obtained from the maximum likelihood algorithm which is used to estimate the parameters. The use of maximum likelihood estimation is described in greater detail below (see §3).

The Topography Product is for those users (oceanographers, geophysicists, and others) who are interested in the height signal from the satellite. The processing chain is shown in figure 2. Apart from the satellite height relative to the sea surface which is produced by the MLE, a number of other parameters and corrections are included. The first of these is the height of the satellite relative to the Earth

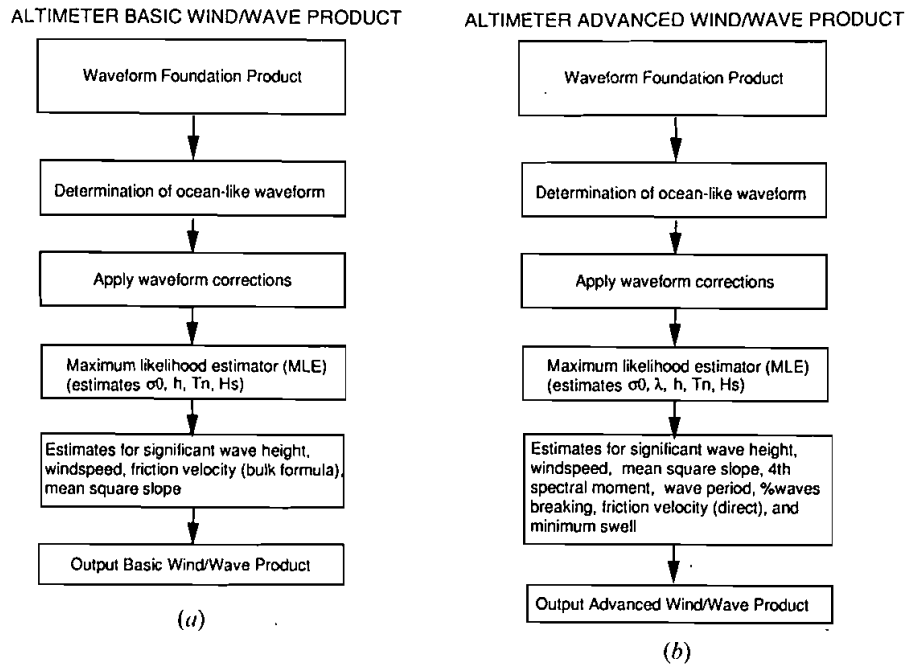


Figure 1. Schematic of the processing chain for the (a) Basic and (b) Advanced Wind/Wave Products.

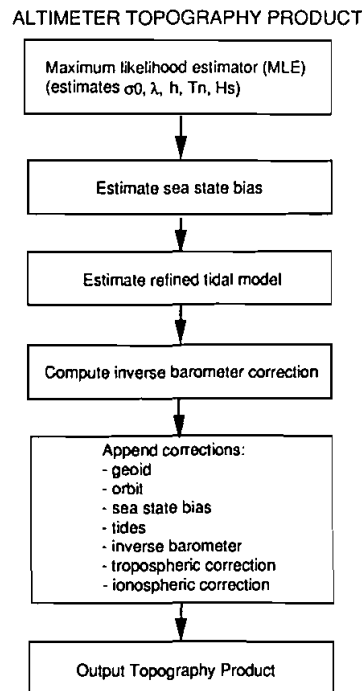


Figure 2. Schematic of the processing chain for the Topography Product.

(essentially, its orbit) derived by tracking. This will be the best available value when the data are processed. The height of the sea surface relative to the reference ellipsoid is calculated from these two values. This is the parameter which, together with geoid information, is used by oceanographers. There are three corrections to account for the effects of the atmosphere on the radar travel time, the dry tropospheric, the wet tropospheric and the ionospheric corrections (Cudlip *et al.* 1994). A sea state bias correction, which corrects for the effect of non-linear surface waves on the ocean, is also calculated. Additionally, there are a number of corrections for sea level changes due to external forcing. There are three tidal corrections, one for the solid earth tide, one for the elastic ocean tide (which includes the ocean loading tide) and the ocean loading tide itself. The final correction is for the so-called inverse barometer effect which is caused by the oceans' response to atmospheric pressure. Details of the processing for the Topography Product is given in §5 below.

In contrast to the approach adopted for previous altimeter missions, the EODC decided to 're-track' the ERS-1 altimeter data. This means that the parameters normally estimated on the satellite (H_s , h and σ^0) are re-estimated on the ground using a 'better' algorithm to analyse the return waveform. There are a number of advantages in this approach. The on-board algorithm is designed to keep the sea surface within the tracking window of the altimeter and thus needs to satisfy two criteria. It needs to be robust and computationally fast. An off-line algorithm on the other hand can be relatively slow computationally, and if a return pulse differs greatly from the expected shape, failure to converge to a solution is a useful quality control tool. Given the removal of computational constraints it is possible to use a much more powerful algorithm than that used on board the satellite. The algorithm chosen for use in the EODC is Maximum Likelihood Estimation (MLE). The algorithm used on board is the SMLE, which stands for Sub-optimal Maximum Likelihood Estimation. The background to the MLE method is given in Challenor and Srokosz (1989) and the implementation is described in §3 below. The MLE is central to the EODC altimeter processing over the ocean. It enables us to produce estimates of the parameters of the waveform that we believe to be statistically optimal and to fit a non-linear version of the Brown model (Srokosz 1986 b). For the Basic Wind/Wave Product and the Topography Product a linear model of the sea surface waves is used, whereas for the Advanced Wind/Wave Product a non-linear wave skewness term is introduced.

The processing scheme has been chosen with the idea of implementing research ideas which have appeared in the literature since the demise of Seasat in 1978. The additional parameters that are being estimated routinely for the first time are mean square slope, wave period, fourth spectral moment, friction velocity, minimum swell height and percentage waves breaking. The aim has been to increase the usefulness of altimeter data to the non-specialist oceanographic user rather than simply to the remote sensing expert.

3. Maximum Likelihood Estimation (MLE)

The maximum likelihood method is a statistical technique of estimating the unknown geophysical parameters from an altimeter return pulse. If a set of noisy data can be described by a model plus a known statistical distribution (Gaussian or otherwise) for the noise, then a maximum likelihood estimator can be used. In certain cases, it can be proved that maximum likelihood is the optimal technique.

The method estimates the parameters by determining which values maximise the probability of obtaining the recorded waveform shape. This maximum is located by differentiating the likelihood function (the product of the probability densities evaluated at each data point) with respect to the unknown parameters and setting the derivatives to zero (Challenor and Srokosz 1989).

From the shape of the return pulse, various geophysical parameters can be determined, significant wave height, normalized radar backscatter, the altitude of the satellite and two non-linear wave parameters, λ and δ . Brown (1977) shows that the average return power as a function of delay is a convolution of the radar system point target response with the average surface response. The average surface response is represented by a convolution of the probability density function of the height of the specular points on the surface with a quantity which depends on the antenna gain and the range from the radar to any point on the scattering surface,

$$P_r(t) = P_{FS}(t)q(\zeta)P_{PT}(t) \quad (1)$$

where $P_{FS}(t)$ is the flat surface response, $q(\zeta)$ is the probability density function of the height of specular points, and $P_{PT}(t)$ is the point target response.

Ulaby *et al.* (1982) have shown that the altimeter radar return power has a negative exponential distribution due to fading noise. If it is assumed that individual pulses are statistically independent, then the average of N pulses will have a gamma, or chi-squared, distribution with N degrees of freedom. Equation 2 shows the likelihood function for an altimeter radar power return (Challenor and Srokosz 1989).

$$\sum_{i=0}^n \left(N \ln N + (N-1) \ln \hat{u}_i - \ln(N-1)! - N \ln u_i - N \frac{\hat{u}_i}{u_i} \right) \quad (2)$$

where \hat{u} represents the observed radar power signal, u represents the model radar signal ((1) plus thermal noise) and is a function of H_s , σ^0 , t_0 , δ , λ , and T_n (the thermal noise), N is the number of pulses averaged (1000 for 1 Hz sampling or 50 for 20 Hz; for ERS-1, the on-board processor averages 50 returns to give 20 Hz data and any further averaging is done during ground processing), and n is the number of 'gates' defined for the instrument (64 for ERS-1). The geophysical parameters for the altimeter are estimated by maximising this expression. The results are described below. It was thought that the mispointing angle of the altimeter instrument, ψ , might be estimated also. Challenor and Srokosz (1989) show that it is not possible to estimate ψ from a single radar return.

The implementation and testing of the MLE required the creation of a set of test data whose characteristics were known. A simulator was developed using (1) to calculate the return power signal delayed over time. Random noise, with the correct statistics, was then superimposed on the signal and the distribution scaled to represent the number of pulses averaged (smaller noise for large N). The test environment can be changed by altering the values of any of the five geophysical parameters or thermal noise.

The MLE was tested with three forms of the return power model. The first contained both non-linear wave parameters, δ and λ . The second estimated the linear terms plus only one non-linear term, λ , with δ set to 0. The last used the linear form with both λ and δ equal to 0. The MLE was run 1000 times for each case, each time changing only the random noise. Table 1 shows the percentage of times each estimated parameter fell within its standard deviation. The theoretical deviation is

Table 1.

Hz	% within 1 theor. std. dev.						% within 1 "real". std. dev.					
	H_s	σ^0	t_0	λ	δ	T_N	H_s	σ^0	t_0	λ	δ	T_N
<i>6 Parameter Fit</i>												
20	5	39	1	17	65	1	66	67	57	65	67	55
1	10	62	6	19	66	8	58	71	57	54	68	59
<i>5 Parameter Fit</i>												
20	13	67	24	21	—	67	56	71	63	58	—	68
1	15	64	22	22	—	66	68	70	67	66	—	68
<i>4 Parameter Fit</i>												
20	33	66	38	—	—	69	67	71	85	—	—	84
1	35	65	37	—	—	67	68	70	85	—	—	84

the deviation determined from the Fisher information matrix for the input values (Challener and Srokosz 1989) and the real standard deviation is determined from the observer Fisher Information matrix (that is, the inverse of the matrix of second derivatives calculated from the MLE estimates). As can be seen in table 1, the percentages are high, over 68 per cent for all four parameters in the linear case. As might be expected, the fits become progressively worse as the model incorporates more non-linear wave parameters; for instance, the percentage of H_s within one theoretical standard deviation drops to 15 per cent when the wave skewness, λ , is added. If both non-linear wave parameters are added, the percentages are even lower.

Theoretically, the MLE should estimate the unknowns fairly well (asymptotically the percentage falling within one theoretical standard deviation should be 68 per cent). The difference in the results for the theoretical and real standard deviations shows that we are a long way from the asymptote. Unfortunately, the numerics of the model equation introduce further complications. To handle the problem numerically, the parameters being estimated need to be scaled to the same order. Given a simple equation such as $y = ax^2 + b$, estimating a and b , the two terms can be scaled to the same order and fitted. But, in a non-linear problem, such as $y = abx^2$, a and b will need to keep the same relative relationship and cannot be scaled to the same order necessarily. Such is the problem with the return power function, the non-linear terms, λ and δ , are very small compared to the other terms which we are estimating. Examples of these fits are shown in figures 3 (six parameter), 4 (five parameter) and 5 (four parameter, linear) for 20 Hz data. The estimated curve for the non-linear fit shows that the amplitude of the curve matches that of the true curve (determined by σ^0 estimate, 6.34 dB estimate and 6.31 dB true), but the corner has a very bad fit because the skewness term λ , affects the slope of the leading edge. This term is very sensitive to the shape of the noise at this point. Better results are obtained for 1 Hz data when the noise is reduced. Although the percentage of estimates that fall within the standard deviations for a parameter are roughly the same for the 20 and 1 Hz data, the standard deviation range is much smaller for the 1 Hz data. For example, for the radar backscatter, σ^0 , the standard deviation is ± 0.15 for the 20 Hz data and

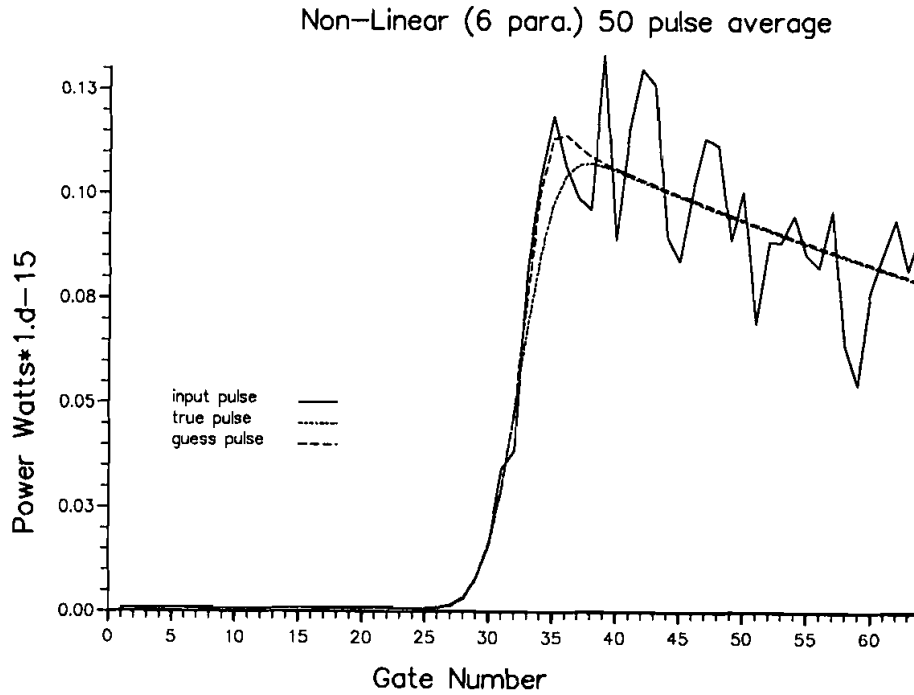


Figure 3. Results for the six parameter MLE fit to a simulated pulse with noise, showing the true solution, the input noisy pulse and the output estimated pulse.

± 0.03 for 1 Hz data. The difference in the error becomes important with σ^0 , from which the wind speed is derived, because at high wind speeds (low σ^0), small errors in the σ^0 value translate to large errors in the wind speed.

Cross-correlation between the six parameters can also be determined. From this information, δ and h are always highly inversely correlated, thus when one is well estimated, the other is incorrectly estimated. In figure 3, δ has a value of -0.56 (true value 0) while t_0 (related to h) is equal to -0.06 nanoseconds, shifting the true curve to the left only slightly. Similarly H_s and λ have a large negative correlation. From our simulations if correlations between parameters are high, then one of the two estimates for the correlated parameters is incorrect.

The results from the six parameter MLE fit described above affect the method of computing the sea state bias using the cross-skewness parameter, δ , and the significant wave height, H_s , suggested by Guymer *et al.* (1985) (see § 5). It has been shown that the cross skewness δ parameter cannot be deconvolved from the height term. Therefore, it will not be possible to compute the sea state bias in this manner.

From the above tests, it has been shown that the 20 Hz data does not produce as accurate results as when averaging the waveforms to 1 Hz. The availability of 20 Hz data will allow narrow features, such as seen by Scott and McDowall (1990) in the Iceland-Faeroes region to be examined in greater detail. An assessment of (i) the degree to which geophysical parameter estimates are degraded, and (ii) whether the 20 Hz data can be used reliably, still awaits the evaluation of the ERS-1 radar altimeter waveform data.

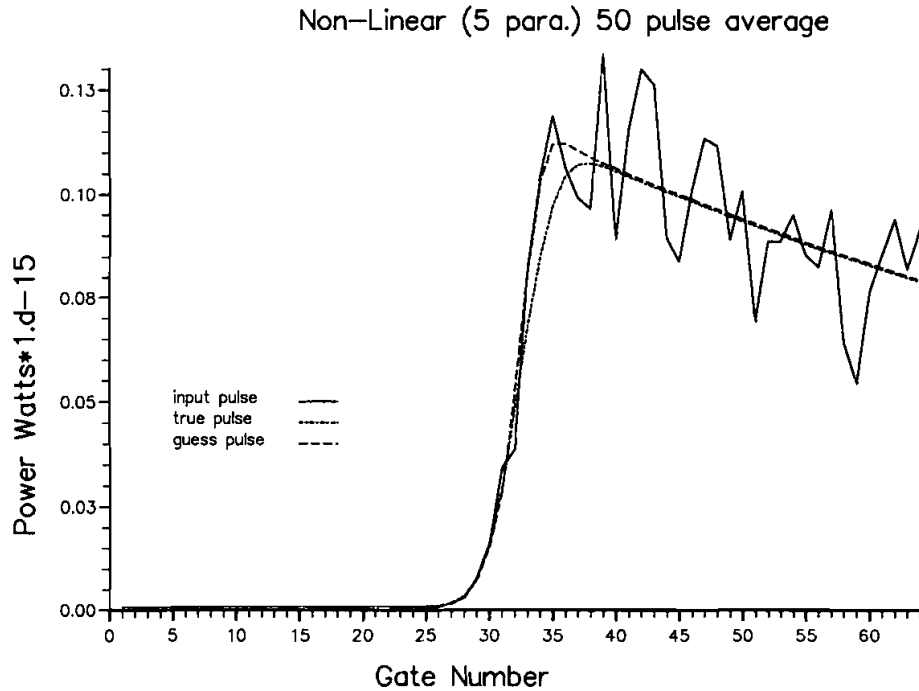


Figure 4. Results for the five parameter MLE fit to a simulated pulse with noise, showing the true solution, the input noisy pulse and the output estimated pulse.

It is not possible to consistently estimate the six parameters from the non-linear model. This is especially true of 20 Hz data. From the figures, the linear model estimates the four parameters, h , H_s , σ^0 , and the thermal noise, well. Of the two nonlinear wave parameters only the wave skewness, λ , can be estimated with the MLE technique, with best results being obtained from the 1 Hz data. (However, for the Advanced Wind/Wave Product it has been decided to process the data at the full resolution of 20 Hz.) The cross-skewness term, δ , cannot be estimated accurately because of its high correlation with h . This concurs with the conclusion found by Rodriguez and Chapman (1991) who estimated λ , from Geosat waveform data, by deconvolving the signal and using a least squares fitting technique. They found that it was necessary to average data for 33 seconds to produce a standard deviation in λ of 0.1. We find slightly better results of a standard deviation of 0.063 for the 1 Hz data. The difference is that Rodriguez and Chapman (1991) used real altimeter data, while we have used simulated data for which, theoretically, the MLE technique should be optimal (Challenor and Srokosz 1989). With a realistic number of pulses used in the average, the MLE technique for the estimation of the geophysical parameters is successful with the linear model, but cannot accurately estimate all the parameters if the non-linear model is used.

4. Wind and wave algorithms

The derivation of significant wave height and wave skewness from the altimeter signal has been described above and in the papers by Brown (1977) and Srokosz

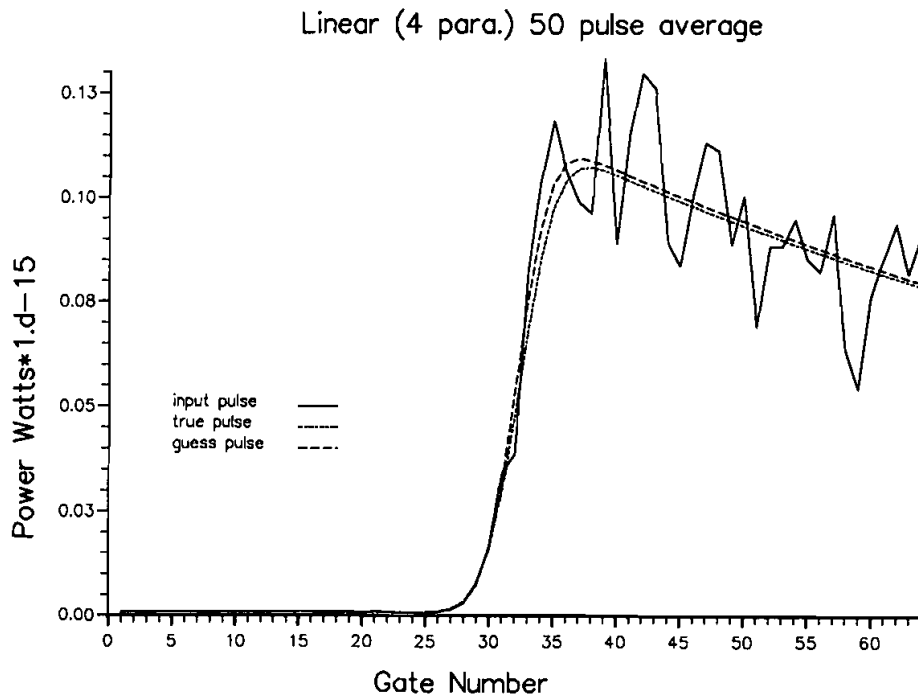


Figure 5. Results for the four parameter (linear) MLE fit to a simulated pulse with noise, showing the true solution, the input noisy pulse and the output estimated pulse.

(1986b). This section will describe the derivation of the other wind and wave parameters in both the Basic and Advanced Wind/Wave Products. The philosophy adopted in the processing of data for the EODC has been wherever possible to use algorithms which have a physical basis rather than those which rely simply on empirical relationships.

The MLE produces estimates of H_s , σ^0 , and for the Advanced Product, λ . The estimates of significant wave height and sea surface skewness need no further processing. A correction is made to σ^0 at this point to account for attenuation of the radar signal by liquid water in the atmosphere.

4.1. Wind algorithms

Unlike the case of significant wave height, we still lack a physical model for the relationship between the mean square slope of the sea surface (or equivalently the normalised radar backscatter cross-section) and the wind speed. This means that we have to base our algorithm on simultaneous measurements of wind speed and altimeter return. Numerous empirical algorithms have been proposed (Brown 1979, Chelton and McCabe 1985, Chelton and Wentz 1986, Witter and Chelton 1991). The algorithm used at the EODC will be based on work by Carter (1990), Carter *et al.* (1991) using Geosat and US NDBO buoy data. Figure 6 taken from Carter *et al.* (1991) shows three different algorithms used for Geosat (σ^0 against wind speed). The point to note here is the close correspondence between Witter and Chelton's and Carter's algorithms. This is quite surprising as they were produced from totally

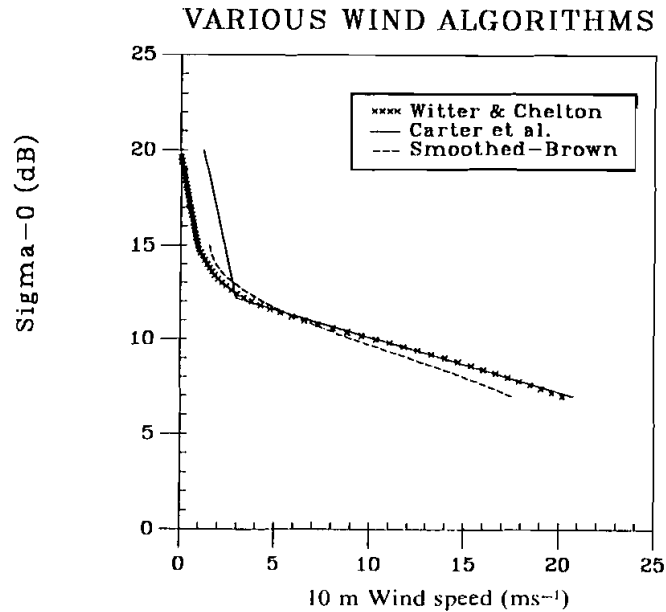


Figure 6. Three algorithms used to derive wind speed from Geosat σ^0 data; $\times \times \times$ Witter and Chelton, — Carter, --- smoothed-Brown.

different data sets. Witter and Chelton compare the wind speed climate from Seasat with Geosat σ^0 s, while Carter uses the comparison with buoy data shown in figure 7. Note, from figure 6, that the smoothed-Brown algorithm recommended for use with Geosat (Goldhirsh and Dobson 1985) differs considerably from the other two and gives poorer estimates of wind speed (Carter *et al.* 1991).

There are two different algorithms to calculate friction velocity. The first, used in the Basic Wind/Wave Product, is to use the 'bulk' formula of Large and Pond (1982). Friction velocity is given by the formula

$$u_* = \sqrt{C_{DN}} U_{10}$$

where C_{DN} is the neutral drag coefficient appropriate to a height of 10 m

$$\begin{aligned} &= 1.14 \times 10^{-3} && 0 < U_{10} < 10 \text{ m s}^{-1} \\ &= (0.49 + 0.065 U_{10}) \times 10^{-3} && 10 \leq U_{10} < 25 \text{ m s}^{-1} \end{aligned}$$

The second (for the Advanced Wind/Wave Product) uses an algorithm similar to that used for wind speed derived from co-incident measurement of wind stress and altimeter σ^0 . Unfortunately to date no such measurements have been made. A joint Remote Sensing Applications Development Unit—James Rennell Centre cruise took place in September 1991 on the RRS *Charles Darwin*, which made such measurements. When these data have been analysed, an algorithm will be calculated and installed at the EODC. In the mean time, both versions of the friction velocity algorithm will use the bulk formula.

4.2. Wave algorithms

The largest increase in the number of parameters produced comes from the field of ocean waves. This is possible because of the scientific advances made in this area,

mostly based on results from Seasat. A brief explanation of each new parameter will be given with its derivation and references.

The mean square slope of the sea surface is related to the normalised radar backscatter cross-section by the formula

$$s^2 = \frac{|R_0^2|}{\sigma^0}$$

where $|R_0^2|$ is the Fresnel reflection coefficient at normal incidence ($=0.617$). This expression was first derived by Barrick (1974).

By transforming the wave spectrum and assuming that the directional spreading function is independent of frequency and has the form $\{\cos(\theta)\}^{2r}$, it is possible to relate the moments of the frequency spectrum to the moments of the wave number spectrum. Transforming the wave spectrum in this way shows M_2 (the second moment of the wave number spectrum) to be equivalent to the fourth moment (m_4) of the frequency spectrum (an early version of this transformation is given in Challenor and Srokosz 1984). The second moment of the wave number spectrum is related to the mean square slope and thus it is possible to compute m_4 from the mean square slope. The formula is

$$m_4 = g^2 \sqrt{s^2} \frac{(r+1)(r+2)}{\sqrt{(2r+1)^2(r^2+r+1)}}$$

where r is the parameter in the directional spreading function of the wave spectrum (Longuet-Higgins *et al.* 1963). Large r implies a narrow spectrum, that is, all the

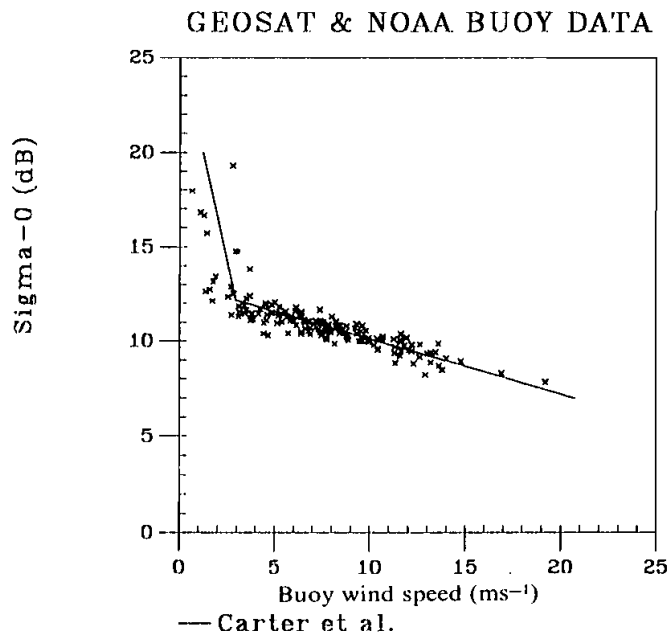


Figure 7. The Carter algorithm —, plotted together with data from Geosat and from NDBO data buoys (+; Geosat σ^0 versus NDBO wind speed).

waves moving in the same direction. In practice, r will vary with both space and time, however for the EODC, a value of $r=8$ has been chosen as a reasonable average.

Given the fourth moment of the wave frequency spectrum and the zeroth moment ($m_0 = H_s^2/16$), it is possible to compute a wave period parameter. The value of the period parameter is given by:

$$T_A = \pi \frac{\sqrt{H_s}}{\sqrt[4]{m_4}}$$

The form of the parameter is different from those normally used in wave work and its value will be smaller than the commonly used zero-upcrossing period, T_z . For details see Challenor and Srokosz (1984, 1991).

The percentage of waves breaking can also be derived using m_4 . The theory behind this parameter is given in Srokosz (1986 a). The percentage is obtained from the formula

$$\text{Percentage Waves Breaking} = \exp\left(\frac{-\kappa^2 g^2}{2m_4}\right)$$

A wave is assumed to break when the downward acceleration at the crest is given by κg . In the EODC implementation of this algorithm $\kappa = 0.4$, as suggested by Srokosz (1986 a).

Conventionally, the ocean wave spectrum can be considered as being divided into two parts corresponding to sea and swell. The sea is that part of the wave spectrum that is generated locally by the wind and in general consists of waves at higher frequencies, whereas swell, which has a longer wavelength, has been generated some distance away and has propagated to the measurement position. If H_s is the total significant wave height then H_{sea} and H_{swell} (the sea and swell heights respectively) are related by

$$H_s^2 = H_{\text{sea}}^2 + H_{\text{swell}}^2$$

As H_s is a measure of the variance of the sea surface elevation (in fact, it is defined as 4 times the standard deviation of the sea surface elevation), this formula represents the total variance as the sum of the variance due to sea and that due to swell (which can, in theory, be related to the wind speed). In a series of papers Mognard (see Mognard 1983, 1984) has generalized maps representing minimum swell in the altimeter measurements of H_s by means of the formula

$$H_{\text{swell}} = \sqrt{H_s^2 - \alpha U_{10}^4}$$

where $\alpha = 6.25$. The term involving the wind speed is the significant wave height for a fully-developed sea. This is when the amount of energy being input by the wind is balanced by dissipation so no more energy can be put into the wave spectrum and thus the waves have ceased to grow. It is therefore the maximum wave height that U_{10} can sustain. H_{swell} is the minimum swell height since we have assumed that the wind sea is at its maximum possible value, which is rarely attained in practice.

5. Ocean topography algorithms

The shape of the sea surface (topography) contains information on currents, tides and bottom features related to solid Earth geophysics. The actual parameter

required from radar altimetry is the elevation of the mean sea surface across each footprint, measured relative to an Earth coordinate system, usually the reference ellipsoid. In addition, for oceanographic studies, it is necessary to know the geoid well, as it is the departure of the sea surface from the geoid that provides information on ocean currents and tides.

To obtain the sea surface topography, it is necessary to measure both the height of the altimeter above the sea surface (range) and the height of the altimeter above the reference ellipsoid (from a precise determination of the orbit). The first is related to a quantity measured by the altimeter itself, that is, the time delay between transmission and reception of pulses, which can be converted to range once the velocity of the pulses is known. However, a number of corrections must be applied to retrieve accurate oceanographic information. These can be divided into three types:

- (i) Propagation corrections which take into account the fact that the velocity of the pulse through the atmosphere differs from that in a vacuum. These are known as the dry tropospheric, wet tropospheric and ionospheric corrections.
- (ii) Corrections for the effect of a non-linear surface wave field, known as the sea state bias.
- (iii) Sea level response corrections, including tides and inverse barometer effect. These are the changes in the sea surface topography induced by physical effects other than the presence of geostrophic currents.

At the EODC, the insertion of the ellipsoid, the geoid and the orbit information into the data stream, and the calculation of the propagation corrections are carried out earlier in the processing, before geophysical parameters are derived (Cudlip *et al.* 1994 this issue). This philosophy contrasts with other altimeter missions, and has been adopted because these quantities are also needed in the processing of ice and land topography at the EODC. The remaining processing steps, (ii) and (iii), are specific to the ocean topography product and are described below.

5.1. Sea state bias

An effect known as sea state bias has been identified from previous missions (see, for example, Born *et al.* 1982, or Fu and Glazman 1991). When fitting model altimeter returns to actual pulses it has usually been assumed that the sea surface is Gaussian. In general this is not the case and a bias results owing to the on-board tracker following the median of the specular points rather than the mean sea level. For Seasat and Geosat empirical determinations of the bias correction of 7 and 2 per cent of H_s were made and recommended for use by users. (The larger value for Seasat was caused by additional errors in the tracker algorithm itself.) However, this assumes that the bias, Δh is related solely to waveheight by a constant, k :

$$\Delta h = kH_s$$

A theoretical approach by Srokosz (1986 b) suggests that the bias also depends on two nonlinear wave parameters, δ the cross-skewness and to a lesser extent λ , the skewness, which are both indicative of sea state development [that is, $k = (\lambda/3 + \delta)/8$]. Thus the correction will vary from pass to pass. Attempts have been made to quantify the effect from analysis of collinear track altimeter data (Guymer and Srokosz 1986, Minster *et al.* 1991). Results show that in wind-wave dominated seas,

k is 2% higher than the values recommended, whereas in swell the values of k are somewhat lower. This uncertainty in sea state bias coefficient would contribute an error of ~ 10 cm to the computation of sea level for waveheights of 4 m. Although the MLE is capable of providing estimates of λ , accurate determination of δ has not proved possible (see § 3 above).

A correction procedure based on multi-pass data is not appropriate in Level 2 processing but could be implemented in higher level processing as part of the estimation of mesoscale variability. The method adopted here is to use the relationship between sea state bias and wave age developed by Glazman and Srokosz (1991) and applied to Geosat data by Fu and Glazman (1991). The wave age ξ characterizes the degree of wave development due to the wind. An estimate of ξ can be made from the altimeter measurements of H_s and U_{10} using (following Fu and Glazman, 1991)

$$\xi = 0.062x^{0.31}$$

where

$$x = 3.4 \times 10^5 g^2 H_s^2 / U_{10}^4$$

then Δh is given by

$$\Delta h = 0.013 (\xi / \xi_m)^{-0.88} H_s$$

where ξ_m ($= 2.3$) is the globally averaged value of ξ (Δh measured in centimetres). It should be noted that the values of the constants in the correction Δh are applicable to Geosat data, being empirically derived (Fu and Glazman 1991), and are in the process of being re-calculated from ERS-1 data to ensure that they are correct.

5.2. Tides

Just as tidal components must be eliminated from current meter measurements when using the data to study ocean circulation, so corrections must be made to altimeter data when inferring geostrophic currents from the measurement of sea level. Neglect of tides in the open ocean will lead to errors of a few tens of cm in ocean topography. There are several different contributions to the tidal signal:

- (i) The body tide, which is the response of the solid earth to the lunar and solar gravitational fields (amplitude ~ 20 cm),
- (ii) The ocean tide which is generally the largest component (~ 100 cm) and is the result of the sun and moon's attraction on the oceans themselves. It can be calculated from quasi-empirical models, in which tide gauge data are used to improve coefficients obtained from hydrodynamical models, or from altimeter data themselves,
- (iii) The loading tide, which arises from the effect of the ocean's loading on the solid Earth and is a few per cent of the ocean tide,
- (iv) Geocentric polar motion which contributes a few centimetres (at present no agreed model exists for this so it is neglected in the correction scheme).

On Seasat and Geosat GDRs only (i) and (ii) were considered. In both cases a Schwiderski-based model (Schwiderski 1980) was used for the ocean tide; that for Seasat had seven constituents (three diurnal and four semidiurnal), while the Geosat scheme included an additional four (one diurnal and three long periods). The Schwiderski model appears to have problems on the U.K. continental shelf (Thomas and Woodworth 1990).

Within the EODC provision has been made for calculating tides at two stages in the processing (Level 1.5 and Level 2; see Cudlip *et al.* 1994, this issue) so that an approximate correction can be included in the Waveform Product for general applications, with a refined, 'state-of-the-art' correction available for the ocean topography product.

Waveform Product Tides. The philosophy used is similar to that for Seasat and Geosat, with the 11-constituent version of Schwiderski being preferred. However, a loading correction has also been incorporated primarily for the altimeter transponder processing. This has been assumed to be 6 per cent of the ocean tide. The algorithm for the Body Tide is similar to the one used for Geosat, with minor modifications for the K1 constituent and its sidebands as proposed by Woodworth (1990).

Ocean Topography Product Tides. The aim is to provide a tidal correction which is as accurate as possible and which is consistent with procedures adopted for processing of the Topex altimeter data (Woodworth 1990). Thus, the loading tide has been added to the ocean tide to give an Elastic Ocean Tide. Tidal models derived from altimeter data automatically include both the loading and the ocean tide so that, if such an approach is selected, the implementation is straightforward. Currently the EODC uses a model based on Geosat data (Cartwright and Ray 1990). In addition to the elastic ocean tide, the loading tide is given separately, based on the work of Cartwright and Ray (1991).

It is worth noting that the ERS-1 altimeter data are not of great use for improving tidal models because its orbit is Sun-synchronous and the choice of 35 days for its main repeat period leads to severe aliasing of the most important tidal constituents.

The algorithm for the Body Tide is identical to that used in the Waveform Product processing (see Cudlip *et al.* 1994, this issue).

5.3. Inverse barometer effect

Atmospheric pressure acting on the surface of the ocean causes changes in sea level additional to those caused by currents. If the response of the ocean is full and instantaneous then the sea level change, Δh (in centimetres), caused by a change in pressure, p , from its mean values, p_0 , is given by the relationship:

$$\Delta h = -\alpha_0(p - p_0)$$

(It should be noted that for the same change in surface pressure this effect is a factor of five larger than that of the dry tropospheric correction.) In general, the ocean is not in equilibrium with atmospheric pressure changes, particularly on short time-scales, and its response depends on the speed with which energy can be radiated away from the region of imposed change (Wunsch 1972). This in turn is affected by the bottom topography.

For EODC processing it has been decided to calculate the full correction using values of pressure passed through from Level 1.5 (Cudlip 1994, this issue). The values of α_0 and p_0 will be obtained from a look-up table. Wunsch (1972) gives $\alpha_0 = 1.01$ and $p_0 = 1013$ mbars; while the recommended values for Geosat (Cheney *et al.* 1987) differed slightly, with $\alpha_0 = 0.9948$ and $p_0 = 1013.3$ mbars. In the EODC processing scheme, p_0 is interpolated from a look-up table containing the mean pressure, in 5° in latitude and 10° in longitude boxes, over the globe (the p_0 value of 1013.3 mbars, used for Geosat, being an estimate of the globally averaged mean

pressure at sea level). This allows for variations in the mean pressure over the surface of the Earth.

6. Applications

6.1. Wind and wave data

Since the launch of Seasat a large amount of work has been done with altimeter wind and wave data. Reviews of this work and some of the possibilities are covered in papers by Carter *et al.* (1988) and Challenor and Srokosz (1991). Here some of the major points are described and some possible directions for the future research are indicated.

Probably the most dramatic use of the Seasat wind/wave data was the article by Chelton *et al.* (1981) which gave a consistent instrumental picture of the global wave climate for the very first time. Previous estimates of the wave climate had relied upon visual observations from ships, with the occasional addition of limited wave buoy data. Challenor *et al.* (1990), Carter *et al.* (1991) and Carter (1990). Carter *et al.* (1991) have extended this work using the Geosat data. Carter *et al.* (1991) have produced monthly climatologies for each year of Geosat's life (1985-1989). Figure 8 shows the contrast between four year for December-January. The variations are dramatic showing drastic changes in the Northern Hemisphere wave climate. By fitting a model of the form

$$H_{si} = A + B \cos(2\pi i/12 + \theta) + C \cos(2\pi i/6 + \phi)$$

where i is an index identifying the month ($i=1$ - no. of months of data), to each 2° square, estimates of seasonal effects can be calculated.

On a more local level Tournadre and Ezraty (1990) have shown that it is possible to derive design heights for off-shore structures from altimeter data. Although Tournadre and Ezraty work in the North Sea, where there is instrumental data to validate their analysis, use of their method with the global wave data from ERS-1 and Geosat will enable design heights to be produced for remote areas of the world without the expense of deploying buoys. Challenor (1982) and Challenor *et al.* (1986) have looked at spatial and temporal scales in the wind and wave fields over the Atlantic Ocean.

Other uses of the data are with wave models. Recently global wave forecasting models have been developed. There are already plans to assimilate altimeter wave height and wind speed data from ERS-1 into such models (Francis and Stratton 1990, Hasselmann *et al.* 1988). Since altimetry provides us with the only global wave data set, it is the only way that these models can be validated on a large scale.

The extra parameters being calculated at the EODC will enable similar analyses to be produced for wave skewness (which tell us about wave non-linearity and whether seas are growing or decaying), wave period, minimum swell and percentage waves breaking (which may give information on gas transfers between the ocean and atmosphere).

6.2. Oceanic mesoscale variability

One of the most successful uses of sea surface topography data obtained by the altimeter has been to calculate the mesoscale variability of the oceanic current systems. Due to the uncertainties in our knowledge of the orbit and the geoid, it has not proved possible to obtain absolute measurements of surface geostrophic currents. This requires a measurement of sea surface slopes with an accuracy of a

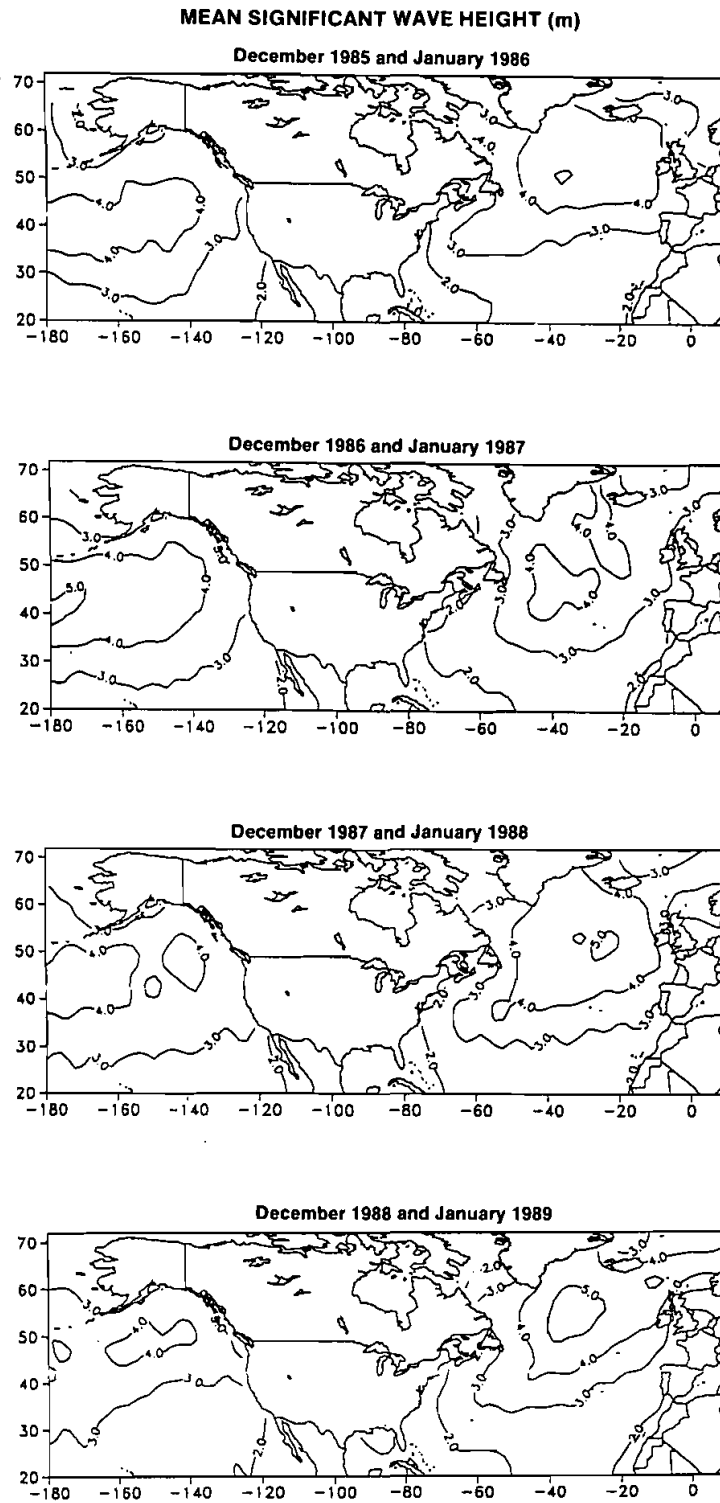


Figure 8. Mean values of the significant waveheight for the months December and January in 1985-6, 1986-7, 1987-8, 1988-9; obtained from Geosat altimeter data.

few centimetres over a hundred kilometres relative to the geoid (slope being related to current via the geostrophic equations; see, for example, Shum *et al.* 1990). While the precision of the altimetric height measurement approaches this requirement, our knowledge of the orbit and geoid do not. Cheney *et al.* (1983) pioneered a method for obtaining the time varying component of the sea surface topography, which shows the variations of the currents about their mean. As these variations are primarily caused by the mesoscale (tens to hundreds of kilometre scale) motions in the oceans, the resulting measurement is called the mesoscale variability.

The Cheney *et al.* (1983) method essentially works by exploiting the fact that the satellite is flying in a repeat orbit. Taking a series of measurements along the same piece of ground track, it is possible to calculate the mean topography, which contains both the geoid and that component of the oceanic current which varies on a time scale longer than that for which the mean is calculated. Subtracting the mean from individual measurements and applying a correction for orbit error allows the variations of the topography about its mean value to be estimated. Figure 9 shows the results of such an analysis as applied to Geosat data in the Agulhas retroflexion region south of Africa, one of the regions of high mesoscale variability in the world's oceans. Here the variability is caused by the shedding of eddies due to the retroflexion of the Agulhas Current flowing south down the east coast of Africa and joining with the Antarctic Circumpolar Current, which flows west to east round Antarctica south of Africa. The figure shows the variability calculated from two years of data. It clearly shows the high variability associated with the eddy shedding

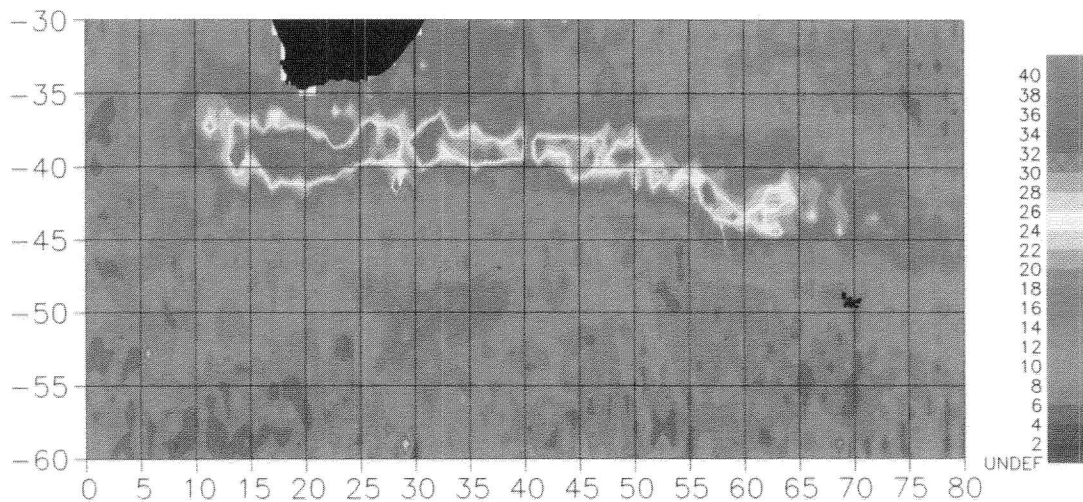


Figure 9. Mesoscale variability (cm) 2 year self variability (December 1986–November 1988), calculated from Geosat altimeter height data, in the Agulhas Retroflexion region to the south and east of Africa. The region of high variability is due to the interaction of the Agulhas Current (flowing south down the east coast of Africa) and the Antarctic Circumpolar Current (flowing west to east round Antarctica).

taking place to the south of Africa. The limitations of this form of analysis are also evident from the figure as there is no direct indication of the presence of the Antarctic Circumpolar Current which has been absorbed into the mean topography. Indirect evidence for the presence of the current is the high variability which then trails off to the east; also the region of somewhat higher variability at 30° E, 50° S shows where the current flows through a gap in the bottom topography, leading again to current fluctuations and, hence, to sea surface variability.

By combining this type of altimetric measurement with other types of data (both *in situ* and remotely-sensed), and with ocean models it is possible to gain a better understanding of the circulation of the world's oceans. The global coverage of the altimeter measurements means that the ocean can be observed in a much more systematic manner than is possible by using ships. In the longer term, assimilation of altimetric data into ocean models may lead to an improved predictive capacity for those models similar to that presently available from atmospheric models.

To conclude this discussion, it is worthwhile to briefly mention some other uses of the altimetric topography measurements over the ocean. These include calculation of the tides, which may be problematical with ERS-1 data due to the satellite's sun-synchronous orbit, (Woodworth and Cartwright 1986) and studies of the marine geoid (Berry *et al.* 1988). The data also allow the use of alternative techniques for extracting information on currents (for example, the cross-over technique; Tai 1988).

6.3. WOCE

The World Ocean Circulation Experiment (WOCE), a part of the World Climate Research Programme, is the largest international study of the physics of the ocean and its role in the Earth's climate (WCRP 1988 (*a*), (*b*)). It is the first attempt to make a coherent, quasi-synoptic survey of the circulation of the world ocean. The U.K. is one of 43 nations participating in WOCE and is planning a substantial contribution, concentrated mainly on the North Atlantic and Southern Ocean (U.K. WOCE 1991).

The 10-year programme has been timed to coincide with a number of satellite missions, particularly ERS-1 and 2 and TOPEX/Poseidon because their payloads include radar altimeters. Maps of the mesoscale eddy field will be obtained using altimeter data, supported by infra-red sea surface temperature measurements. These will provide a context for ship and buoy measurements. The latter will give only intermittent coverage of portions of ocean basins, but the satellite data will allow spatial and temporal variations over a wide range of scales to be studied. Eddy statistics derived from altimeter data will also be used to validate dynamical models of the ocean and to guide their future development.

The geoid contained within the EODC ocean topography product is not accurate enough to permit determination of the mean ocean circulation, an important quantity required in the estimation of ocean heat transport. However, during the 1990s, there is the prospect of a satellite mission to determine independently the surface gravity field and geoid. Once this has been achieved, the improved geoid can be applied retrospectively to the ERS-1 altimeter data.

The WOCE data set will benefit ERS-1 by providing high quality *in situ* data for validation purposes. In the altimetric context, the important measurements are those related to sea level/currents from CTD, current meter and bottom pressure recorders

and surface wind velocity and stress estimates from ship and buoy meteorological packages.

6.4. Calibration and validation

Clearly, those who will make use of the data products, for various applications, will want some assurance as to the quality of the data. For this reason, associated with each of the three products described in this paper will be validation products that compare the altimetric data with *in situ* measurements. Such data will come from a variety of sources (too varied to be fully described here), and will enable the accuracy of the geophysical parameters to be assessed. A major contribution to the calibration and validation of the products will come from data collected for other purposes; for example, wave data obtained by offshore operators, or data from oceanographic experiments such as WOCE (see §6.3 above). Additional data will be obtained from the ESA wind/wave calibration/validation experiment that took place off the coast of Norway in the autumn of 1991, and other dedicated measurements. These data are being processed and compared with the ERS-1 altimeter oceans products, so that the quality of the products can be assessed.

The authors of this paper, along with other colleagues, were involved in a research cruise which took place in September 1991, near the Faeroes, on the RRS *Charles Darwin*. The aim being to obtain *in situ* data for the calibration and validation of ERS-1 measurements. Using a combination of buoy and ship-based measurement techniques, data on waves, winds, surface stress, currents, sea surface temperature and the hydrography of the region were obtained, mostly along the satellite ground tracks in the region. These are now being analysed and are being compared to ERS-1 data, as they become available.

Summary

This paper has given an overview of the oceans processing scheme for ERS-1 altimeter data at the U.K. EODC. In contrast to the processing philosophy adopted for previous altimetric missions, a single product (the Geophysical Data Record or GDR) has not been produced. Instead, three products (the basic and advanced wind/wave products, and the topography product) are being produced, with the aim of serving a wider user community. Central to the processing scheme is the use of MLE to analyse the altimeter waveforms to derive accurate geophysical data. Additionally, the derivation of a number of new geophysical parameters is included in the processing, again the overall aim being to provide the user with the maximum amount of useful geophysical information.

Acknowledgments

We are grateful to David Carter of IOSDL for providing figures 6, 7 and 8, and to Graham Quartly of RSADU for providing figure 9. Some of this work was supported under a contract awarded by the Defence Research Agency.

References

- BARRICK, D. E., 1972, Remote sensing of sea-state by radar, chapter 12 in *Remote sensing of the troposphere*, edited by V. E. Derr (Washington DC: U.S. Government Printing Office).

- BARRICK, D. E., 1974, Wind dependence of quasi-specular microwave sea scatter. *I.E.E.E. Transactions on Antennas and Propagation*, **AP-22**, 449-454.
- BARRICK, D. E., and LIPA, B. J., 1985, Analysis and interpretation of altimeter sea echo, *Advanced Geophysics*, **27**, 60-99.
- BERRY, P. A. M., MEADOWS, A. J., ALLAN, T. D., and OLLIVER, J. G., 1988, A comparison of reduction methods for satellite altimetry data. *Geophysical Journal*, **95**, 63-68.
- BORN, G. H., RICHARDS, M. A., and ROSBOROUGH, G. W., 1982, An empirical determination of the effects of sea state bias on Seasat altimetry. *Journal of Geophysical Research*, **87**, 3221-3226.
- BROWN, G. S., 1977, The average impulse response of a rough surface and its applications. *I.E.E.E. Transactions on Antennas and Propagation*, **AP-25**, 67-74.
- BROWN, G. S., 1979, Estimation of surface winds using satellite-borne radar measurements at normal incidence. *Journal of Geophysical Research*, **84**, 3974-3978.
- CARTER, D. J. T., 1990, Development of procedures for the analysis of ERS-1 radar altimeter wind and wave data using Geosat data. European Space Agency Study Report under Contract 8315/89/HGE-1.
- CARTER, D. J. T., CHALLENGOR, P. G., and SROKOSZ, M. A., 1988, Satellite remote sensing and wave studies into the 1990s. *International Journal of Remote Sensing*, **9**, 1835-1846.
- CARTER, D. J. T., FOALE, S., and WEBB, D. J., 1991, Variations in global wave climate throughout the year. *International Journal of Remote Sensing*, **12**, 1687-1697.
- CARTWRIGHT, D. E., and RAY, R. D., 1990, Oceanic tides from Geosat-ERM altimetry. *Journal of Geophysical Research*, **95**, 3069-3090.
- CARTWRIGHT, D. E., and RAY, R. D., 1991, Energetics of global ocean tides from Geosat altimetry. *Journal of Geophysical Research*, **96**, 16,897-16,912.
- CHALLENGOR, P. G., 1982, Spatial variations of significant waveheight. In *Satellite Microwave Remote Sensing*, edited by T. D. Allan (Chichester: Ellis Horwood Ltd), pp. 451-460.
- CHALLENGOR, P. G., and SROKOSZ, M. A., 1984, Extraction of wave period from altimeter data. *Proceedings of the Workshop on ERS-1 Radar Altimeter Data Products*, **ESA SP-221**, (Noordwijk, The Netherlands: ESA), pp. 121-124.
- CHALLENGOR, P. G., and SROKOSZ, M. A., 1989, The extraction of geophysical parameters from radar altimeter return from a nonlinear sea surface. In *Mathematics in Remote Sensing*, edited by S. R. Brooks (Oxford: Clarendon Press), pp. 257-268.
- CHALLENGOR, P. G., and SROKOSZ, M. A., 1991, Wave studies with the radar altimeter. *International Journal of Remote Sensing*, **12**, 1671-1686.
- CHALLENGOR, P. G., FOALE, S., and WEBB, D. J., 1990, Seasonal changes in the global wave climate measured by the Geosat altimeter. *International Journal of Remote Sensing*, **11**, 2205-2213.
- CHALLENGOR, P. G., GUYMER, T. H., and SROKOSZ, M. A., 1986, The influence of spatial and temporal scales on calibration/validation. *Proceedings of the Workshop on ERS-1 Wind and Wave Calibration*, **ESA SP-262**, (Noordwijk, The Netherlands: ESA), pp. 11-16.
- CHELTON, D. B., and MCCABE, P. J., 1985, A review of satellite altimeter measurements of sea surface wind speed: with a proposed new algorithm. *Journal of Geophysical Research*, **90**, 4707-4720.
- CHELTON, D. B., and WENTZ, F. J., 1986, Further development of an improved altimeter wind speed algorithm. *Journal of Geophysical Research*, **91**, 14,250-14,260.
- CHELTON, D. B., HUSSEY, K. J., and PARKE, M. E. 1981, Global satellite measurements of water vapour, wind speed and wave height. *Nature*, **294**, 529-532.
- CHENEY, R. E., MARSH, J. G., and BECKLEY, B. D., 1983, Global mesoscale variability from collinear tracks of Seasat altimeter data. *Journal of Geophysical Research*, **88**, 4343-4354.
- CHENEY, R. E., DOUGLAS, B. C., AGREEN, R. W., MILLER, L., PORTER, D. L., and DOYLE, N. S., 1987, Geosat altimeter geophysical data record user handbook, NOAA Technical Memorandum NOS NGS-46 (Rockville, MD: NOAA).
- CUDLIP, W., and MILNES, M., 1994, Overview of altimeter data processing at the EODC. *International Journal of Remote Sensing*, **15**, 871-887.
- CUDLIP, W., MANTRIPP, D. R., GRIFFITHS, H. D., SHEEHAN, D. V., WRENCH, C. L., LESTER, M., LEIGH, R. P., and ROBINSON, T. R., 1994, Corrections for altimeter low-level processing at the EODC. *International Journal of Remote Sensing*, **15**, 889-914.

- FRANCIS, P. E., and STRATTON, R. A., 1990, Some experiments to investigate the assimilation of Seasat altimeter waveheight data into a global wave model. *Quarterly Journal of the Royal Meteorological Society*, **116**, 1225-1251.
- FU, L.-L., and GLAZMAN, R. E., 1991, The effect of the degree of wave development on the sea state bias in radar altimetry measurements. *Journal of Geophysical Research*, **96**, 829-834.
- GLAZMAN, R. E., and SROKOSZ, M. A., 1991, Equilibrium wave spectrum and sea state bias in satellite altimetry. *Journal of Physical Oceanography*, **21**, 1609-1621.
- GOLDHIRSH, J., and DOBSON, E. B., 1985, A recommended algorithm for the determination of ocean surface wind speed using a satellite-borne radar altimeter. Report SIR85U-005, Johns Hopkins APL.
- GUYMER, T. H., and SROKOSZ, M. A., 1986, The determination of sea-state bias and nonlinear wave parameters from satellite altimeter data. *ESA/EARSeL Symposium on Europe from Space*, **ESA SP-258**, (Noordwijk, The Netherlands: ESA), pp. 115-120.
- GUYMER, T. H., CHALLENGOR, P. G., SROKOSZ, M. A., RAPLEY, C. G., QUEFFEULOU, P., CARTER, D. J. T., GRIFFITHS, H. D., MCINTYRE, N. F., SCOTT, R. F., and TABOR, A. R., 1985, A Study of ERS-1 Radar Altimeter Data processing Requirements, Wormley Institute of Oceanographic Sciences, Report No. 220.
- HASSELMANN, K., HASSELMANN, S., BAUER, E., BRUNING, C., LEHNER, S., GRABER, H., and LIONELLO, P., 1988, Development of a satellite SAR image spectra and altimeter wave height data assimilation system for ERS-1. European Space Agency Study Report under Contract 6875/87/HGE-I(C) [also Max Planck Institute for Meteorology, Report No. 19].
- HAYNE, G. S., and HANCOCK, D. W., 1990, Corrections for the effects of significant wave height and attitude on Geosat radar altimeter measurements, *Journal of Geophysical Research*, **95**, 2837-2842.
- LARGE, W. G., and POND, S., 1982, Sensible and latent heat flux measurements over the ocean. *Journal of Physical Oceanography*, **12**, 464-482.
- LIPA, B. J., and BARRICK, D. E., 1981, Ocean surface height-slope probability density function from SEASAT altimeter echo, *Journal of Geophysical Research*, **86**, 10921-10930.
- LONGUET-HIGGINS, M. A., CARTWRIGHT, D. E., and SMITH, N. D., 1963, Observations of the directional spectrum of sea waves using the motion of a floating buoy. *Proceedings of Conference on Ocean Wave Spectra* (Englewood Cliffs, NJ: Prentice Hall), pp. 111-132.
- MINSTER, J-F., JOURDAN, D., BOISSIER, C., and MIDOL-MONNET, P., 1991, Estimation of the sea state bias in radar altimeter Geosat data using a short arc technique. *Journal of Atmospheric and Oceanic Technology*, **9**, 174-187.
- MOGNARD, N. M., 1983, Swell propagation in the North Atlantic Ocean using Seasat altimeter. In *Satellite Microwave Remote Sensing*, edited by T. D. Allan (Chichester: Ellis Horwood Ltd), pp. 425-437.
- MOGNARD, N. M., 1984, Ocean wave parameters extraction using satellite short-pulse radar altimeters. *Proceedings of the Workshop on ERS-1 Radar Altimeter Data Products*, **ESA SP-221**, (Noordwijk, The Netherlands: ESA), pp. 37-42.
- PETERS, E. R., PLUMB, K., and VECK, N. J., 1994, ERS-1 Product Generation at the EODC. *International Journal of Remote Sensing*, **15**, 733-740.
- RODRIGUEZ, E., and CHAPMAN, B., 1991, Ocean skewness and the skewness bias in altimetry: a Geosat Study. Submitted to *Journal of Geophysical Research*.
- SCHWIDERSKI, E. W., 1980, Global ocean tides, 1: A detailed hydrodynamical interpolation model. *Marine Geodesy*, **3**, 161-217.
- SCOTT, J. C., and MCDOWALL, A. L., 1990, Cross-frontal cold jets near Iceland: in-water, satellite infrared, and Geosat altimeter data. *Journal of Geophysical Research*, **95**, 18005-18014.
- SHUM, C. K., WERNER, R. A., SANDWELL, D. T., ZHANG, B. H., NEREM, R. S., and TAPLEY, B. D., 1990, Variations of global mesoscale eddy energy observed from Geosat. *Journal of Geophysical Research*, **95**, 17,865-17,876.
- SROKOSZ, M. A., 1986a, On the probability of wave breaking in deep water. *Journal of Physical Oceanography*, **16**, 382-385.
- SROKOSZ, M. A., 1986b, On the joint distribution of surface elevation and slopes for a nonlinear random sea, with an application to radar altimetry. *Journal of Geophysical Research*, **91**, 995-1006.

- TAI, C-K., 1988, Geosat crossover analysis in the tropical Pacific. 1. Constrained sinusoidal crossover adjustment. *Journal of Geophysical Research*, **93**, 10,621-10,629.
- THOMAS, J. P., and WOODWORTH, P. L., 1990, The influence of ocean tide model corrections on Geosat mesoscale variability maps of the North East Atlantic. *Geophysical Research Letters*, **17**, 2389-2392.
- TOURNADRE, J., and EZRATY, R., 1990, Local climatology of wind and sea state by means of satellite radar altimeter measurements. *Journal of Geophysical Research*, **95**, 18255-18268.
- UK WOCE, 1991, *Ocean Circulation and Climate*, edited by D. Smythe-Wright (Swindon: NERC).
- ULABY, F. T., MOORE, R. K., and FUNG, A. K., 1982, *Microwave remote sensing: active and passive*, Volume II (Reading, Mass.: Addison-Wesley).
- WCRP, 1988 a, *World Ocean Circulation Experiment Implementation Plan*, Volume I, Detailed Requirements, WCRP-11 (WMO/TD No. 242) (Geneva: WMO).
- WCRP, 1988 b, *World Ocean Circulation Experiment Implementation Plan*, Volume II, Scientific Background, WCRP-12 (WMO/TD No. 243) (Geneva: WMO).
- WITTER, D. L., and CHELTON, D. B., 1991, A method for developing an altimeter wind speed algorithm with application to Geosat. *Journal of Geophysical Research*, **96**, 8853-8860.
- WOODWORTH, P. L., 1990, Specification of Topex/Poseidon Tide Algorithms, Topex/Poseidon Tides Subcommittee Report (unpublished report).
- WOODWORTH, P. L., and CARTWRIGHT, D. E., 1986, Extraction of the M2 ocean tide from Seasat altimeter data. *Geophysical Journal of the Royal Astronomical Society*, **84**, 227-255.
- WUNSCH, C., 1972, Bermuda sea level in relation to tides, weather, and baroclinic fluctuations. *Reviews of Geophysics*, **10**, 1-49.